Spin-Coupled Description of Aromaticity in the Retro Diels−Alder Reaction of Norbornene†

J. Grant Hill,‡,§ David L. Cooper,*,|| and Peter B. Karadakov*,‡

Department of Chemistry, University of York, Heslington, York, YO10 5DD, and Department of Chemistry, University of Liverpool, Liverpool, L69 7ZD, United Kingdom

Received: February 1, 2008; Revised Manuscript Received: June 18, 2008

The electronic rearrangements along the lowest-energy path for the gas-phase retro Diels−Alder reaction of norbornene are monitored using spin-coupled theory. We find that the most dramatic changes to the electronic structure occur in a relatively narrow interval in which the system passes through a geometry at which it can be considered to be significantly aromatic. We provide an estimate of the vertical resonance energy. Our results are consistent with the anticipated synchronous "aromatic" nature of this reaction, but we find that the key changes occur a little before the actual transition state is reached.

1. Introduction

It is now widely accepted that the gas-phase retro Diels−Alder reaction of norbornene, leading to cyclopentadiene and ethene, occurs via a concerted mechanism, at least in the absence of radical-stabilizing substituents. Although femtosecond experiments[1] initially raised the possibility of a stepwise process, involving biradical intermediates, it is now well-established that the lowest energy thermal pathway on the ground-state potential energy surface is instead of the synchronous "aromatic" type.[2–6]

The purpose of the present work is to show whether and how such "aromatic" character is revealed by modern valence bond (VB) theory in its spin-coupled (SC) form. The basic methodology is much the same as in a number of previous studies of gas-phase organic reaction pathways, in which we examined the form of the SC wave function, and the values of several associated quantities, at various points along an appropriate intrinsic reaction coordinate (IRC).[7–12] In the case of electrocyclic reactions,[8–11] many of these studies have resulted in fairly similar "homolytic" electronic mechanisms involving transition states (TSs) at which the SC wave functions attain strong resemblance to the well-known modern VB description of the paragon of aromaticity, benzene.[13] On the other hand, a number of other such studies have led to various different descriptions.[11] It would, though, be very surprising indeed if the present study suggested an electronic mechanism that was significantly different from that of the parent Diels−Alder reaction between butadiene and ethene, the SC description of which provided the first example of a "homolytic" combination of parallel bond-breaking and bond-formation processes passing through an "aromatic" TS.[8]

The structure of this paper is as follows. In the next section, we outline briefly the computational methodology. We then present our results, which do indeed show very clearly the anticipated synchronous "aromatic" character of the electronic mechanism of the retro Diels−Alder reaction of norbornene, and provide an estimate of the vertical resonance energy, albeit with the most dramatic changes in the wave function occurring a little before the TS is reached. Finally, we present a summary and our overall conclusions.

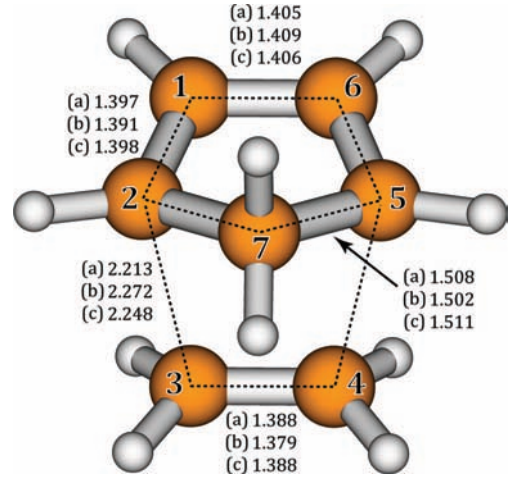

Figure 1. Optimized carbon−carbon bond lengths for the TS: (a) CCSD(Full)/6-31G(d), (b) MP2(Full)/6-31G(d), and (c) B3LYP/6-31G(d). Also shown is our numbering scheme for the carbon atoms.

2. Computational Methodology

All geometry, frequency, and IRC calculations were carried out in C_s symmetry with the GAUSSIAN03 package,[14] at the B3LYP, MP2(Full), and CCSD(Full) levels, within a standard 6-31G(d) basis set, using the very tight convergence criteria and including all electrons in the MP2 and CCSD treatments. We checked that all of the TS geometries were characterized by a single negative eigenvalue of the Hessian.

SC calculations were then performed within the same basis set, at selected points along the IRC calculated at the B3LYP/6-31G(d) level with a step size of 0.1 amu$^{1/2}$ bohr. The SC(6) wave function used here can be written in the form[15]

$$\Psi_{\mathrm{SC}} = \hat{A}\left[\left(\prod_{i=1}^{23}\phi_i\alpha\phi_i\beta\right)\left(\prod_{\mu=1}^{6}\psi_\mu\right)\Theta_{00}^{6}\right] \qquad (1)$$

in which the ψ_μ are nonorthogonal one-electron "active" SC orbitals, which are optimized simultaneously with the orthogonal doubly occupied "inactive" orbitals ϕ_i, and with Θ_{00}^{6}. This last is the (optimized) active-space total spin function for the spins

† Part of the "Sason S. Shaik Festschrift".

* To whom correspondence should be addressed. E-mail: dlc@liverpool.ac.uk (D.L.C.) and pbk1@york.ac.uk (P.B.K.).

‡ University of York.

§ Present address: School of Chemistry, Cardiff University, Park Place, Cardiff CF10 3AT, U.K.

|| University of Liverpool.

10.1021/jp800969k CCC: $40.75
Published on Web 09/17/2008

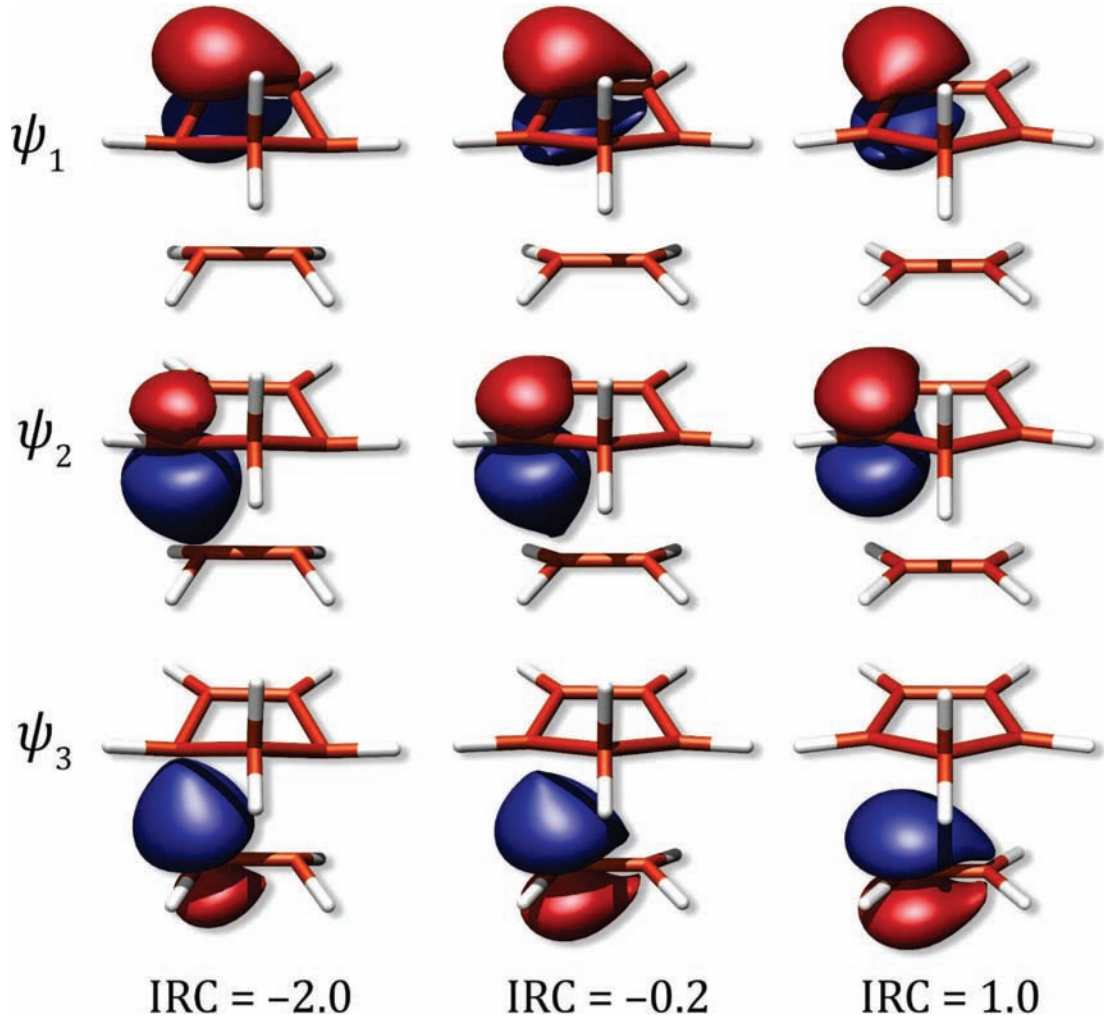

Figure 2. Snapshots of symmetry-unique SC orbitals along the B3LYP/6-31G(d) IRC segment: left-hand column, −2.0 amu$^{1/2}$ bohr (closest to norbornene); middle column, −0.2 amu$^{1/2}$ bohr (a little before the TS); and right-hand column, +1.0 amu$^{1/2}$ bohr (toward cyclopentadiene and ethene). Three-dimensional iso-value surfaces corresponding to $\psi_\mu = \pm 0.08$ were obtained from POV-Ray (Persistence of Vision Raytracer) files produced by MOLDEN.[28]

of six electrons coupled to a net singlet, and it is expressed as a linear combination of a full set of all five linearly independent modes of spin coupling:

$$\Theta^6_{00} = \sum_{k=1}^{5} C_{0k}\Theta^6_{00;k} \tag{2}$$

in which C_{0k} are termed the spin-coupling coefficient. The calculations described here were carried out in the Kotani spin basis,[16,17] which is native to the SC code that we employed,[18] but the values of C_{0k} were transformed[19] to those for the Rumer basis,[16,20] which proves more convenient when analyzing the evolution of the wave function during the course of this particular reaction. The importance or "weights" in Θ^6_0 of the five different modes of spin coupling are quantified here using the scheme of Chirgwin and Coulson.[21] These Chirgwin−Coulson weights are examined alongside the forms of the SC orbitals and the overlaps between them.

Some additional insight into the changes to the SC wave function along the IRC is provided by plots of the Wiberg−Mayer indices,[22,23] defined according to

$$W_{AB} = \sum_{p\in A}\sum_{q\in B}(\mathbf{DS})_{pq}(\mathbf{DS})_{qp} \tag{3}$$

in which **D** is the total spin-less one-particle density matrix, **S** is a corresponding overlap matrix, and the notation $p \in A$ signifies all basis functions centered on atom *A*. Such quantities can be expected to show points of inflection in the region of the IRC where the bonding pattern is changing most rapidly,[23] even if absolute values of W_{AB} tend not to be especially informative for correlated wave functions.

We also performed standard B3LYP/6-311+G(d,p) calculations of nucleus-independent chemical shift (NICS) values[25,24] for various geometries along the B3LYP/6-31G(d) IRC. For the purposes of direct comparison, we also carried out various calculations (at the same levels of theory) for the parent Diels−Alder reaction between butadiene and ethene.[26]

3. Results and Discussion

The carbon−carbon bond lengths in the TS geometries, optimized at various levels of theory, are summarized in Figure 1, which also shows the numbering scheme adopted for the carbon atoms. Except for the two interfragment bond lengths, the differences between the results from the various approaches are fairly small. We observe for the interfragment distances that the B3LYP/6-31G(d) results are closer to those from CCSD(Full)/6-31G(d) than are the numbers obtained using MP2(Full)/6-31G(d).

We also examined the thermochemistry output that is provided by GAUSSIAN03 frequency calculations on the reactants, products, and TSs. The various values, including

activation enthalpies and entropies for the forward and reverse reactions, are in harmony with those that have been reported in other studies.[4–6] In spite of possible concern over the predicted strain of the norbornene framework,[6] it turns out that B3LYP/6-31G(d) does fairly well in predicting thermochemical activation data. Branchadell[4] found that values obtained at the B3LYP level for the potential energy barrier were very close to those obtained with QCISD(T)/6-31G(d), whereas perturbation theory up to third order (i.e., MP3) was required. All in all, on the basis of our own results, as well as those in the literature, it seems appropriate for this system to use B3LYP/6-31G(d) in preference to MP2(Full)/6-31G(d) for generating the IRC.

The evolution of the SC orbitals along the B3LYP/6-31G(d) IRC is summarized in Figure 2 by means of snapshots of the symmetry-unique orbitals ψ_1, ψ_2, and ψ_3. Reflection of these three orbitals in the C_s mirror plane generates ψ_6, ψ_5, and ψ_4, respectively. At −2.0 amu$^{1/2}$ bohr, which is the end of the IRC segment closest to norbornene, orbitals ψ_2 and ψ_3 are clearly involved in a bonding interaction that is reminiscent of a classical σ type bond. An equivalent σ type bond arises from ψ_4 and ψ_5, whereas orbitals ψ_1 and ψ_6 are involved in the expected π type bond. By −0.2 amu$^{1/2}$ bohr, near to the TS, the SC orbitals show signs of mutation toward the forms that will eventually pertain to the products. For example, although ψ_1 is clearly still involved in a π type interaction with ψ_6, there is now also a notable tail toward ψ_2. Orbitals ψ_2 and ψ_3 have taken on greater $2p_\pi$ character, but each of them shows bulges in the direction of both adjacent SC orbitals. At +1.0 amu$^{1/2}$ bohr, where the IRC segment heads toward the products, these transformations are fairly complete, with ψ_1 and ψ_2, and similarly ψ_5 and ψ_6, forming π type bonds in the cyclopentadiene moiety, while ψ_3 and ψ_4 constitute the π type bond in ethene.

Summarizing these observations, we can say that the bonds involving ψ_2 and ψ_3, ψ_4 and ψ_5, and ψ_1 and ψ_6 on the norbornene side of the TS are broken at much the same time as the bonds involving ψ_1 and ψ_2, ψ_3 and ψ_4, and ψ_5 and ψ_6 are being formed. This is of course what we would expect for a concerted "homolytic" mechanism, but tracking the forms of these orbitals corresponds to just one part of analyzing the changes to the SC wave function along the IRC. In particular, we also need to examine the weights of the different modes of spin coupling.

The composition of the active-space spin-coupling pattern along the IRC is illustrated in Figure 3a. At −2.0 amu$^{1/2}$ bohr, the total active-space spin function is dominated by a single Rumer eigenfunction ($k = 4$), consistent with the expected bonding pattern in norbornene. At +1.0 amu$^{1/2}$ bohr, on the product side of the TS, the most important Rumer spin function is instead the one with $k = 1$, consistent with the bonding in separate cyclopentadiene and ethene fragments. In between these two extremes, we observe that the most dramatic change from one pattern to the other occurs over a relatively narrow region, a little before the TS. These two Rumer functions, with $k = 1$ and $k = 4$, are analogous to the Kekulé modes of spin coupling in benzene[13] but adapted to the atomic framework of this particular reaction. Similarly, the other three Rumer functions, whose weights remain fairly small all the way along this IRC segment, are analogues of the Dewar type modes in benzene.

It is clear from Figure 3a that the Chirgwin−Coulson weights of the two Kekulé-like modes become equal on the norbornene side of this IRC segment, a little before −0.2 amu$^{1/2}$ bohr is reached. A similar displacement from the TS is seen in Figure 3b, which shows the evolution along the IRC of the nearest-

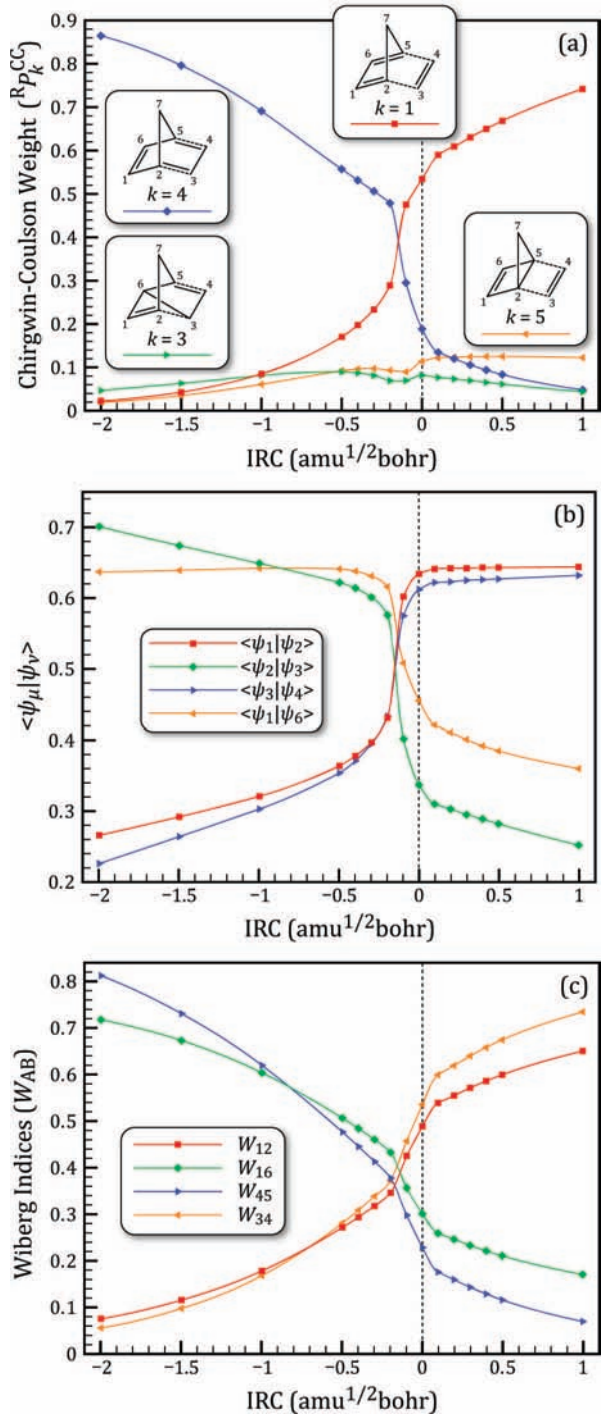

Figure 3. Evolution of key quantities along the B3LYP/6-31G(d) IRC: (a) Chirgwin−Coulson weights ($^{R}P_k^{CC}$) of the Rumer modes of spin coupling (the $k = 2$ and $k = 3$ Rumer modes are related by symmetry and have equal weights); (b) nearest-neighbor overlaps $\langle\psi_\mu|\psi_\nu\rangle$ between SC orbitals; and (c) Wiberg−Mayer indices W_{AB} for neighboring carbon atoms.

neighbor overlaps between SC orbitals. The most rapid changes between the values of overlap integrals characteristic of the reactants to those characteristic of the products occur over a very narrow region of the IRC. The shapes of the various curves in Figure 3, parts a and b, are of course entirely consistent with our expectations for the synchronous making and breaking of bonds and the associated recoupling of the electron spins, except that the fastest changes appear to occur a little before the TS. We will return later to this apparent "displacement" from the

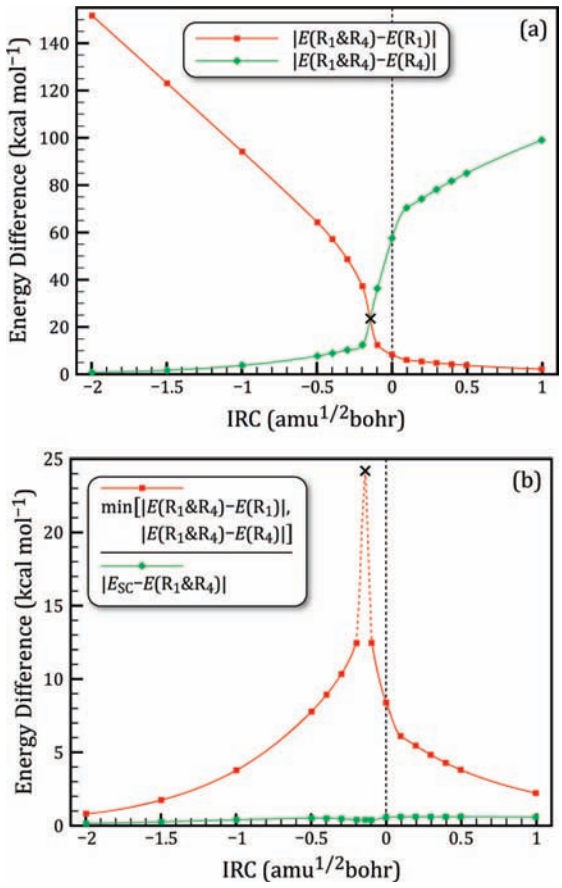

Figure 4. Variations of energy differences along the IRC, as defined in the text. (a) $|E(R_1\ \&\ R_4) - E(R_1)|$ & $|E(R_1\ \&\ R_4) - E(R_4)|$; (b) $\min[|E(R_1\ \&\ R_4) - E(R_1)|, |E(R_1\ \&\ R_4) - E(R_4)|]$, and $|E_{SC} - E(R_1\ \&\ R_4)|$. The interpolated parts of the left- and right-hand branches of the first of these curves (shown as dashed lines) cross at $E(R_1) = E(R_4)$.

TS geometry of the major electronic structure changes, which are already fairly complete by the time the TS is reached. Slightly more gradual changes from reactant to products are observed in the generalized Wiberg−Mayer indices for neighboring carbon atoms (see Figure 3c), but we notice again that various curves have points of inflection, and indeed cross, in the same general region as do the weights of the Kekulé type modes and also the nearest-neighbor orbital overlaps.

A number of factors in the SC results presented so far combine to suggest benzene-like aromaticity in a relatively narrow region along the IRC: the spin-coupling pattern resembles that in ground-state benzene, certain nearest-neighbor overlap integrals become equal, certain Wiberg−Mayer indices become equal, and even the shapes of the SC orbitals (middle column of Figure 2) are reminiscent to some extent of those for benzene.[13] Of course, one of the energetic criteria for aromaticity in a system such as this one is the demonstration of a sizable resonance energy arising from the involvement of the two Kekulé-like Rumer eigenfunctions. Perhaps the most obvious way of estimating this resonance energy is to evaluate the separate energies, at the same geometries and with fixed orbitals (coming from the fully variational SC wave function), of each of the two Kekulé-like modes and also of the variationally optimized combination of the two of them. Denoting these various fixed-orbital energies as $E(R_1)$, $E(R_4)$, and $E(R_1\ \&\ R_4)$, it proves useful to look at the absolute differences $|E(R_1\ \&\ R_4) - E(R_1)|$ and $|E(R_1\ \&\ R_4) - E(R_4)|$. The smaller of these two quantities at any given geometry gives an indication of the energy lowering that can be achieved for

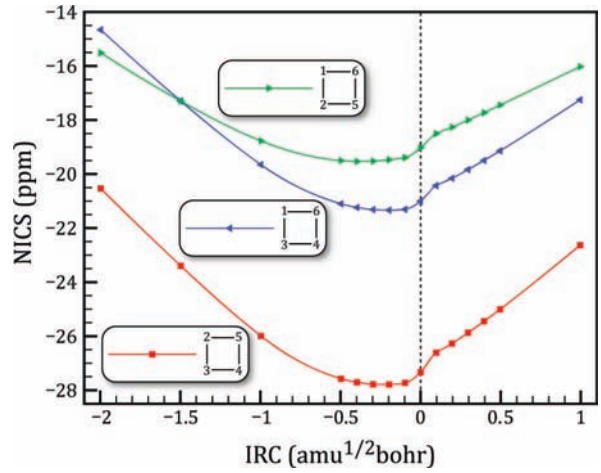

Figure 5. Evolution of B3LYP/6-311+G(d,p) NICS parameters for the retro Diels−Alder reaction of norbornene along the B3LYP/6-31G(d) IRC segment. (a) CCSD(Full)/6-31G(d), (b) MP2(Full)/6-31G(d), and (c) B3LYP/6-31G(d). Also shown is our numbering scheme for the carbon atoms.

the "more important" Kekulé type mode by allowing it to mix with the "less important" one. This quantity thus serves as a useful indication of the vertical resonance energy. We could instead have chosen to use the full SC energy, E_{SC}, instead of $E(R_1\ \&\ R_4)$, but it turns out that $|E_{SC} - E(R_1\ \&\ R_4)|$ remains fairly small for all of the geometries we considered, never reaching 0.61 kcal mol^{-1}.

The values of $|E(R_1\ \&\ R_4) - E(R_1)|$ and $|E(R_1\ \&\ R_4) - E(R_4)|$ along the IRC are shown in Figure 4a, and the smaller of these two quantities at any given geometry (i.e., our estimate of the vertical resonance energy) is replotted in Figure 4b together with $|E_{SC} - E(R_1\ \&\ R_4)|$. We have denoted by a cross the position at which $E(R_1) = E(R_4)$, according to interpolations based on rational functions in continued fraction form. This procedure suggests a maximum resonance energy of 24.2 kcal mol^{-1} close to -0.139 amu$^{1/2}$ bohr. The analogous definition based on E_{SC} instead of $E(R_1\ \&\ R_4)$ suggests a maximum of 24.5 kcal mol^{-1} at almost the same position along the IRC. These estimates of the resonance energy are larger than those that we observed for the parent Diels−Alder reaction between butadiene and ethene.[8,26] Indeed, they are larger than the corresponding value for the ground-state of benzene.[13]

Taken together, the various quantities that we have described here leave little doubt that a modern VB description, in SC form, of the retro Diels−Alder reaction of norbornene indicates a narrow region of the IRC, a little before the TS, at which we can recognize aromatic character during the synchronous making and breaking of bonds. The apparent small shift of this key region away from the TS can be attributed to the combined effect of several factors that can influence the arrangement of the six carbon atoms participating in the bond-breaking and bond-making processes required to achieve aromatic behavior. To start with, there are obvious steric interactions involving the methylene group from the cyclopentadiene fragment, while another important factor is associated with the fact that the SC calculations are performed on top of an IRC calculated by means of a different approach, which has a different balance between nondynamic and dynamic correlation effects. The SC wave function emphasizes the nondynamic correlation effects between the electrons involved in the bonding rearrangements, which explains why the maximum in E_{SC} along the B3LYP/6-31G(d) IRC also occurs a little before the TS, at very much the same position as that of the maximum vertical resonance energy.

Displacements of the most "aromatic" structure along the IRC away from the TS have also been found to occur in the SC descriptions of other reactions, starting with the disrotatory electrocyclic ring-opening of cyclohexadiene.[9] In addition to this, displacements of this type have been observed and discussed in other VB studies of chemical reaction mechanisms.[27]

Interestingly, it turns out that certain NICS values for geometries along the B3LYP/6-31G(d) IRC, calculated without any reference to our SC wave functions, also exhibit minima that are slightly shifted to the norbornene side of the TS. We show in Figure 5 NICS values calculated at the B3LYP/6-311+G(d,p) level of theory for the rings formed by carbon atoms (1,2,5,6), (1,3,4,6), and (2,3,4,5), with the atoms numbered as in Figure 1. The minima in these curves confirm the small displacement of the most aromatic structure to a geometry a little before the TS established through the analysis of the SC wave function.

Our NICS value (−27.8 ppm) for the TS of the retro Diels−Alder reaction of norbornene, calculated in the center of the main overlap region [the (2,3,4,5) ring] between the two fragments, turns out to be slightly lower than the corresponding value (−25.3 ppm) for the TS in the parent Diels−Alder reaction between butadiene and ethene.[26] Including only π contributions, the NICS value for the ground-state of benzene is −20.7 ppm.[25] These various observations do of course parallel those mentioned earlier in relation to our estimates of the vertical resonance energy. On the other hand, as is well-known, NICS values are relatively insensitive for a system such as benzene to geometrical distortions that significantly diminish the degree of aromaticity. As such, it is not at all surprising that the curves displayed in Figure 5 differ from those in Figures 3 and 4 in the sense of not showing any particularly dramatic changes over a narrow region of the IRC.

4. Summary and Conclusions

The electronic rearrangements that occur along the lowest-energy path for the gas-phase retro Diels−Alder reaction of norbornene have been monitored by means of a series of SC(6)/6-31G(d) calculations along the B3LYP/6-31G(d) IRC. We examined the evolution along this pathway of the shapes of the SC active orbitals, the overlaps between them, the Chirgwin−Coulson weights of the different Rumer modes of spin coupling, values of generalized Wiberg−Mayer indices for neighboring carbon atoms, and an estimate of the vertical resonance energy. We also calculated NICS values at the B3LYP/6-311+G(d,p) level of theory.

We find that each SC orbital remains semilocalized on a single atomic center throughout the course of the reaction, with distortions toward nearest neighbors that reflect the particular bonding situation and with the corresponding recoupling of the electron spins. The electronic mechanism revealed by the present study closely resembles that of the parent Diels−Alder reaction of butadiene and ethene,[8,26] and it is tempting to denote the various rearrangements with half arrows:

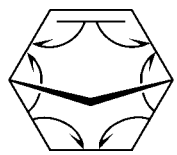

It is important to stress that this "homolytic" representation is not in any sense meant to suggest a biradical mechanism: Our examination of the evolution of the SC wave function along the IRC shows that the bond-making and bond-breaking processes occur in concert over a relatively short interval of the IRC. Within this region, the system passes through a geometry at which it can be considered to be significantly aromatic. Our estimate of the vertical resonance energy, ca. 24.2 kcal mol^{-1}, is larger than the corresponding value for the parent Diels−Alder reaction, and indeed, it is larger than that in benzene. We observe that the most dramatic changes along the B3LYP/6-31G(d) IRC segment occur a little before the actual TS is reached.

Supporting Information Available: Tables of the numerical data used to construct Figures 3−5. This material is available free of charge via the Internet at http://pubs.acs.org.

References and Notes

(1) Horn, B. A.; Herek, J. L.; Zewail, A. H. *J. Am. Chem. Soc.* **1996**, *118*, 8755.

(2) (a) Houk, K. N.; Loncharich, R. J.; Blake, J. F.; Jorgensen, W. L. *J. Am. Chem. Soc.* **1989**, *111*, 9172. (b) Jorgensen, W. L.; Lim, D.; Blake, J. F. *J. Am. Chem. Soc.* **1993**, *115*, 2936.

(3) (a) Beno, B. R.; Wilsey, S.; Houk, K. N. *J. Am. Chem. Soc.* **1999**, *121*, 4816. (b) Wilsey, S.; Houk, K. N.; Zewail, A. H. *J. Am. Chem. Soc.* **1999**, *121*, 5772. (c) Diau, E. W.-G.; De Feyter, S.; Zewail, A. H. *Chem. Phys. Lett.* **1999**, *304*, 134. (d) Singleton, D. A.; Schulmeier, B. E.; Hang, C.; Thomas, A. A.; Leung, S.-W.; Merrigan, S. R. *Tetrahedron* **2001**, *57*, 5149.

(4) Branchadell, V. *Int. J. Quantum Chem.* **1997**, *61*, 381.

(5) Dinadayalane, T. C.; Vijaya, R.; Smitha, A.; Narahari Sastry, G. *J. Phys. Chem. A* **2002**, *106*, 1627.

(6) Guner, V.; Khuong, K. S.; Leach, A. G.; Lee, P. S.; Bartberger, M. D.; Houk, K. N. *J. Phys. Chem. A* **2003**, *107*, 11445.

(7) (a) Blavins, J. J.; Cooper, D. L.; Karadakov, P. B. *Int. J. Quantum Chem.* **2004**, *98*, 465. (b) Blavins, J. J.; Cooper, D. L.; Karadakov, P. B. *J. Phys. Chem. A* **2004**, *108*, 914.

(8) Karadakov, P. B.; Cooper, D. L.; Gerratt, J. *J. Am. Chem. Soc.* **1998**, *120*, 3975.

(9) Karadakov, P. B.; Cooper, D. L.; Thorsteinsson, T.; Gerratt, J. In *Quantum Systems in Chemistry and Physics. Volume 1: Basic Problems and Models Systems*; Hernández-Laguna, A., Maruani, J., McWeeny, R., and Wilson, S. Eds.; Kluwer: Dordrecht, 2000; pp 327−344.

(10) (a) Cooper, D. L.; Karadakov, P. B.; Thorsteinsson, T. In *Valence Bond Theory*; Cooper, D. L. Ed.; Elsevier: Amsterdam, 2002; pp 41−53. (b) Blavins, J. J.; Cooper, D. L.; Karadakov, P. B. *J. Phys. Chem. A* **2005**, *109*, 231.

(11) (a) Karadakov, P. B.; Cooper, D. L.; Gerratt, J. *Theor. Chem. Acc.* **1998**, *100*, 222. (b) Karadakov, P. B.; Cooper, D. L. *J. Phys. Chem. A* **2001**, *105*, 10946. (c) Blavins, J. J.; Karadakov, P. B.; Cooper, D. L. *J. Org. Chem.* **2001**, *66*, 4285. (d) Blavins, J. J.; Karadakov, P. B.; Cooper, D. L. *J. Phys. Chem. A* **2003**, *107*, 2548. (e) Hill, J. G.; Karadakov, P. B.; Cooper, D. L. *Theor. Chem. Acc.* **2006**, *115*, 212. (f) Karadakov, P. B.; Hill, J. G.; Cooper, D. L. *Faraday Discuss.* **2007**, *135*, 285.

(12) Blavins, J. J.; Cooper, D. L.; Karadakov, P. B. *J. Phys. Chem. A* **2004**, *108*, 194.

(13) Cooper, D. L.; Gerratt, J.; Raimondi, M. *Nature* **1986**, *323*, 699.

(14) Frisch, M. J.; Trucks, G. W.; Schlegel, H. B.; Scuseria, G. E.; Robb, M. A.; Cheeseman, J. R.; Montgomery, J. A.; Vreven, T.; Kudin, K. N.; Burant, J. C.; Millam, J. M.; Iyengar, S. S.; Tomasi, J.; Barone, V.; Mennucci, B.; Cossi, M.; Scalmani, G.; Rega, N.; Petersson, G. A.; Nakatsuji, H.; Hada, M.; Ehara, M.; Toyota, K.; Fukuda, R.; Hasegawa, J.; Ishida, M.; Nakajima, T.; Honda, Y.; Kitao, O.; Nakai, H.; Klene, M.; Li, X.; Knox, J. E.; Hratchian, H. P.; Cross, J. B.; Adamo, C.; Jaramillo, J.; Gomperts, R.; Stratmann, R. E.; Yazyev, O.; Austin, A. J.; Cammi, R.; Pomelli, C.; Ochterski, J. W.; Ayala, P. Y.; Morokuma, K.; Voth, G. A.; Salvador, P.; Dannenberg, J. J.; Zakrzewski, V. G.; Dapprich, S.; Daniels, A. D.; Strain, M. C.; Farkas, O.; Malick, D. K.; Rabuck, A. D.; Raghavachari, K.; Foresman, J. B.; Ortiz, J. V.; Cui, Q.; Baboul, A. G.; Clifford, S.; Cioslowski, J.; Stefanov, B. B.; Liu, G.; Liashenko, A.; Piskorz, P.; Komaromi, I.; Martin, R. L.; Fox, D. J.; Keith, T.; Al-Laham, M. A.; Peng, C. Y.; Nanayakkara, A.; Challacombe, M.; Gill, P. M. W.; Johnson, B.; Chen, W.; Wong, M. W.; Gonzalez, C.; Pople, J. A. *Gaussian 03*, Revision B.03; Gaussian, Inc.: Pittsburgh, PA, 2003.

(15) (a) Cooper, D. L.; Gerratt, J.; Raimondi, M. *Chem. Rev.* **1991**, *91*, 929. (b) Gerratt, J.; Cooper, D. L.; Karadakov, P. B.; Raimondi, M. In *Handbook of Molecular Physics and Quantum Chemistry*; Wilson, S. Ed.; Wiley: Chichester, 2003; Vol. 2, Part 2, Chapter 12, pp 148−168.

(16) Pauncz, R. *Spin Eigenfunctions*; Plenum Press: New York, 1979.

(17) Kotani, M.; Amemyia, A.; Ishiguro, E.; Kimura, T. *Tables of Molecular Integrals*; Maruzen: Tokyo, 1963.

(18) Karadakov, P. B.; Gerratt, J.; Cooper, D. L.; Raimondi, M. *J. Chem. Phys.* **1992**, *97*, 7637.

(19) Karadakov, P. B.; Gerratt, J.; Cooper, D. L.; Raimondi, M. *Theor. Chim. Acta* **1995**, *90*, 51.

(20) Rumer, G. *Göttinger Nachr.* **1932**, *3*, 337.

(21) Chirgwin, B. H.; Coulson, C. A. *Proc. R. Soc. London, Ser. A* **1950**, *201*, 196.

(22) (a) Wiberg, K. N. *Tetrahedron* **1968**, *24*, 1083. (b) Mayer, I. *Chem. Phys. Lett.* **1983**, *97*, 270.

(23) Ponec, R.; Yuzhakov, G.; Cooper, D. L. *J. Phys. Chem. A* **2003**, *107*, 2100, and references therein.

(24) Schleyer, P. v. R.; Maerker, C.; Dransfield, A.; Jiao, H.; Hommes, N. J. v. E. *J. Am. Chem. Soc.* **1996**, *118*, 6317.

(25) Jiao, H.; Schleyer, P. v. R. *J. Phys. Org. Chem.* **1998**, *11*, 655.

(26) Hill, J. G. Ph.D. Thesis, University of York, UK, 2005.

(27) See, for example, (a) Song, L.; Wu, W.; Dong, K.; Hiberty, P. C.; Shaik, S. *J. Phys. Chem. A* **2002**, *106*, 11361. (b) Su, P.; Song, L.; Wu, W.; Hiberty, P. C.; Shaik, S. *J. Am. Chem. Soc.* **2004**, *126*, 13539.

(28) Schaftenaar, G.; Noordik, J. H. *Comput. Aided Mol. Des.* **2000**, *14*, 123.

JP800969K